Supporting Information

Self-evolving persistent luminescence nanoprobe for autofluorescence-free ratiometric imaging and on-demand enhanced chemodynamic therapy of pulmonary metastatic tumors

Xu Zhao [*a,b,c], Tian-Yue Gu [a,b,c], You-Peng Xia [a,b,c], Xue-Mei Gao[d], Li-Jian Chen [a,b,c], Li-Xia Yan [a,b,c] and Xiu-Ping Yan [a,b,c,d]

[a] State Key Laboratory of Food Science and Resources, Jiangnan University, Wuxi 214122, China

[b] International Joint Laboratory on Food Safety, Jiangnan University, Wuxi 214122, China

[c] Institute of Analytical Food Safety, School of Food Science and Technology, Jiangnan University, Wuxi 214122, China

[d] Key Laboratory of Synthetic and Biological Colloids, Ministry of Education, School of Chemical and Material Engineering, Jiangnan University, Wuxi 214122, China

*Email: zhaoxu2017@jiangnan.edu.cn

Supplementary Methods

Chemicals and Materials. Germanium oxide (GeO_2), manganese nitrate ($Mn(NO_3)_2$), zinc nitrate ($Zn(NO_3)_2$), cupric nitrate ($Cu(NO_3)_2$), sodium hydroxide (NaOH), *N, N*-dimethylformamide (DMF), ammonium hydroxide ($NH_3 \cdot H_2O$ 25%~28%), cetyltrimethyl ammonium bromide (CTAB), alcohol (MeOH, 99.7%), ethanol (EtOH), cyclohexane (CYH, 99.7%), cyclohexane, chloroform, dimethyl sulfoxide (DMSO), and methylene blue (MB) were bought from Sinopharm Chemical Reagent Co. Ltd. (Shanghai, China). Zinc acetylacetonate hydrate ($Zn(acac)_2 \cdot xH_2O$,97%), gallium acetylacetonate ($Ga(acac)_3$), $Cr(acac)_3$ (97%), 1-octadecene (ODE, 90%), oleic acid (OA, 85%), (3-Mercaptopropyl)trimethoxysilane (MPTES, 97%), ethyl orthosilicate, glutathione (GSH, 98%), 5,5'-dithiobis-(2nitrobenzoic acid) (DTNB), and 2',7'-dichlorodihydrofluorescein diacetate (DCFH-DA) were purchased from Aladdin (Shanghai, China). DSPE-PEG_{2000}-Mal was supplied by Xi'an Ruixi Biological Technology Co., Ltd (Xi'an, China). 3-(4,5-Dimethyl-thiazol-2-yl)-2,5diphenyltetrazolium bromide (MTT) was purchased from Macklin Co. Ltd. (Shanghai, China). 4',6-diamidino-2-phenylindole (DAPI) was purchased from Beyotime Biotechnology Co. (Shanghai, China). Calcein acetoxymethyl ester and propidium iodide (Calcein-AM/PI) live and dead bacteria detection kit were supplied from Yeason Biotechnology Co. (Shanghai, China). Penicillin-streptomycin, fetal bovine serum (FBS), Dulbecco's modified Eagle's high glucose medium (DMEM), and other consumables for cell culture were obtained from Dingguo Biotechnology Co. Ltd. (Beijing, China). High-purity water was supplied

by Hangzhou Wahaha Group Co. Ltd (Hangzhou, China). All reagents were of at least of analytical grade and used without further purification.

Instrumentation and characterization. Fourier transform infrared (FT-IR) spectra were carried out on a Nicolet IS50 spectrometer (Thermo, America) by using KBr pellet. X-ray diffraction (XRD) spectra were obtained from a D2 PHASER diffractometer (Bruker AXS, Germany). Phosphorescence and fluorescence spectra were performed on an F-7000 spectrofluoro photometer (Hitachi, Japan). Absorption spectra were recorded on a UV 3600 PLUS UV-Vis- NIR spectrometer (Shimadzu, Japan). Transmission electron microscopy images (TEM) were obtained at 200 kV with a JEM-2100 TEM (JEOL, Japan). Zeta potential and hydrodynamic size distribution were measured on a ZEN3700 Nano laser particle size analyzer (Marvin, England). Electron spin resonance (ESR) images were determined by EMXplus-10/12 spectrometer (Bruker, Germany). Cell imaging was acquired on a FV3000 confocal laser scanning microscope (CLSM) (Olympus, Japan). Absorbance for the MTT assay was recorded on a Synergy H1 microplate reader (BioTek, USA) at a wavelength of 490 nm. *In vivo* phosphorescence imaging of mice was carried out on an IVIS Lumina III imaging system (PerkinElmer, America). Blood routine examination was carried out using Automated Hemotology Analyzer (BC-5000 Vet, China).

Preparation of persistent luminescence nanoparticles ZGMC, ZGC, ZGM and magnetic nanoparticles MNPs.

Zn_2GeO_4:Mn/Cu (ZGMC) was prepared consulted previous methods with several adjustments.[1,2] Briefly, $Zn(NO_3)_2$ (6 mmol), $Mn(NO_3)_2$ (15 μmol), $Cu(NO_3)_2$ (6 μmol)

were dispersed in H_2O in a round-bottom flask and stirred vigorously. Then, 900 μL HNO_3 was added, followed by Ge(Ⅳ) (3 mmol) added dropwise, which was pre-made according to previous work.[3] After the addition of 48 mg CTAB, the pH of the solution was adjusted to 9.0 with $NH_3 \cdot H_2O$. By the end of a 1-hour stirring, the solution was transferred into Teflon-lined autoclaves and kept at 220℃ for 6 h. After cooling to room temperature, the mixture was collected by centrifugation and washing by H_2O and EtOH. After cooling to room temperature, the mixture was collected by centrifugation and washing by EtOH and H_2O. Finally, the product ZGMC was lyophilized and stored for further use.

$ZnGa_2O_4$:Cr (ZGC) was synthesized referring to previous articles along with a slight modification.[4,5] Generally, 0.358 g $Zn(acac)_2 \cdot xH_2O$ and 0.734 g $Ga(acac)_3$ were dispersed in 50 mL ODE and 40 mL OA, heated and mixed at 80℃ until dissolved completely. 1.4 mg $Cr(acac)_3$ was added into the solution while $Cr(acac)_3$ was pre-dissolved in MeOH and the solution was cooled down to 40-50℃, followed with the addition of 10 mL MeOH. Then, the solution was transferred into Teflon-lined autoclaves and kept at 220℃ for 24 h. After cooling to room temperature, the mixture was collected by centrifugation and washing by EtOH and cyclohexane (v:v=1:1). Finally, the product ZGC was dried at room temperature under vacuum and stored for further use.

Zn_2GeO_4:Mn (ZGM) was prepared with reference to the previous literature[2]. And MNPs was prepared consulting to preceding work[6].

The preparation of functionalized ZGMC-SH, ZGC-Mal and MNPs-SH.

The thiol functionalized ZGMC (ZGMC-SH) was synthesized according to preceding studies.[2] 1 mg ZGMC was ultrasonically scattered in 1 mL NaOH (5 mM) and stirred for 24 h at room temperature. The product ZGMC-OH was collected by centrifugation, washed by H_2O and EtOH and obtained after frozen-dried overnight. Then, 2 mg ZGMC-OH was dispersed in 1 mL DMF, while 8 μL MPTES was added drop by drop. The solution was vigorously stirred at 80℃ for 24 h, centrifuged and washed by DMF and EtOH. Subsequently, ZGMC-SH was collected after being vacuum-dried overnight.

To prepare ZGC-Mal, a two-step ligand modification method was conducted, according to previous studies.[5] 1 mg ZGC was dispersed in 0.25 mL chloroform along with 0.5 mg DSPE-PEG_{2000}-Mal, and stirred at 60℃ overnight. After 0.25 mL H_2O was added into the mixture while the reaction ended, the vacuum spinning procedure was performed at 70℃ to remove the chloroform. The mixture was centrifuged and washed by EtOH for twice and by H_2O for once and frozen-dried overnight. The intermediate product was collected, and went through the same procedure as the former one. At this point, the product ZGC-Mal was completed acquired.

MNPs-SH was synthesized according to former researches with slight adjustments. [6] 150 mg of Fe_3O_4 nanospheres were weighed and dispersed in 100 mL of ethanol. After sonication for 30 min, 25 mL of H_2O and 1.2 mL of $NH_3 \cdot H_2O$ were added with 100 μL of ethyl orthosilicate and 5 mL of EtOH under mechanical stirring. The reaction could last for 9 h. The obtained particles were collected with a magnet and washed three times with ethanol and water. The above product was dispersed in

120 mL of isopropanol and 0.5 mL of MPTES was added. after mechanical stirring for 9 h, the product was separated and washed with H_2O and EtOH, and then dried in a vacuum oven overnight.

Fabrication of ZGMC@ZGC-TAT:

4 mg ZGC-Mal was ultrasonically dispersed in 4 mL PBS (pH 8.0), and 1 mg ZGMC was added, when the phosphorescence intensity of the solution at 537 nm and 700 nm were equal roughly. After stirred for 6 hours, 1 mg MNPs-SH was added to combine with excessive ZGC-Mal, and the stirring continued overnight. The resultant ZGMC@ZGC was separated by magnetic separation and washed with H2O.

The prepared ZGMC@ZGC was dispersed in PBS (pH 8.0) along with TAT of equal weight and blended overnight. The final product was washed by H_2O and collected after frozen-drying.

Acid degradation properties of ZGMC@ZGC-TAT:

The acid degradation properties of ZGMC@ZGC-TAT are investigated through several indicators including phosphorescence intensity, luminescence images, and morphology, by fluorescence spectrophotometer, IVIS Lumina III imaging system, and TEM, separately. Phosphorescence intensity of ZGMC and ZGMC@ZGC-TAT (0.6 mg mL^{-1}), which were dispersed in PBS buffer solution (pH 6.0, 6.5, and 7.4), were detected at different time points (0, 1, 2, 3, 4, 5, 6, 8, and 24 h, respectively).

Luminescence images of 100 μL of above solutions (n=3) were captured in a black 96-well plate after a 10-min irradiation of a UV lamp (6 W), which were taken at different time points (0, 1, 2, 3, 4, 5, 6, 8, and 24 h, respectively).

In order to study the morphology changes of ZGMC and ZGMC@ZGC-TAT, TEM samples were prepared by 10 μL of ZGMC and ZGMC@ZGC-TAT (0.6 mg mL^{-1}) dispersed in PBS buffer solution (pH 6.0 and pH 7.4), at different time points (0, 3, 6, and 24 h, respectively) and further photographed.

CDT properties of ZGMC@ZGC-TAT:

The CDT features of ZGMC and ZGMC@ZGC-TAT were manifested through the release of ions. ZGMC and ZGMC@ZGC-TAT (0.6 mg mL^{-1}) were prepared in PBS buffer solution (pH 6.0, pH 6.5, and pH 7.4, respectively), 1 mL of which were taken out at different time points (0, 1, 2, 3, 4, 5, 6, 8, 24 h, respectively). The Mn^{2+} and Cu^{2+} concentrations of above solutions were detected by ICP-MS.

The depletion of GSH was analyzed by the DTNB probe. While ZGMC@ZGC-TAT solution prepared in PBS buffer solution (pH 6.0 and pH 7.4) mixed with GSH (10 mmol L^{-1}) and shaken for different times (0, 0.5, 1, 1.5, 2, 3, 4, 5, 6 h), 100 μL mixture supernatant was collected following centrifugation. DTNB (15 mol L^{-1}) resolved in PBS (pH 7.4) and 100 μL mixture supernatant were added into a 96-well plate. The absorbance values at 410 nm were recorded after solution incubated for 10 min. In addition, the absorbance values (at 410 nm) of other solutions at different times were detected: 1) GSH; 2) GSH +ZGMC (pH 6.0); 3) GSH + ZGMC (pH 7.4).

The enhanced CDT effect was measured with TMB as ROS indicator. ZGMC@ZGC-TAT (0.6 mg mL^{-1}) were mixed with TMB (0.5 mmol L^{-1}), H_2O_2 (10 mmol L^{-1}) and GSH (10 mmol L^{-1}) and then oscillated in an acidic environment. UV spectra were obtained for the supernatant of the mixture after 1 h. Besides, the spectrums

of other groups were detected: 1) TMB + H_2O_2; 2) TMB + H_2O_2+ ZGM; 3) TMB + H_2O_2+ ZGMC; 4) TMB + H_2O_2 + GSH; 5) TMB + H_2O_2 + GSH + ZGM; 6) TMB + H_2O_2 + GSH + ZGMC. The pH-responsive generation of ·OH was detected by the UV-Vis spectrum variations of the MB probe. PBS solutions (pH 6.0) with MB (20 mg L^{-1}), H_2O_2 (20 mmol L^{-1}), $NaHCO_3$ (50 mmol L^{-1}), and ZGMC@ZGC-TAT (500 μg mL^{-1}) was shaken after 6 h and the spectrum of their supernatant between 400 nm and 800 nm were detected by a UV-Vis spectrophotometer. In addition, the spectrums of other solutions were detected: 1) MB+ $NaHCO_3$; 2) MB+ H_2O_2+ $NaHCO_3$. What's more, above solutions were taken out at different time points (0, 0.5, 1, 1.5, 2, 2.5, 3, 3.5, 4, 5, 6 h) and centrifugated for supernatant, the absorbance at 664 nm of which were measured.

***In vitro* ratio imaging characteristic validation:**

To evaluate the cell uptake of ZGMC@ZGC-TAT, the mouse squamous cell carcinoma cell line (SCC-7) was employed as a cell model and seeded into a confocal capsule (1 × 10^5 cell per capsule). With a 24 h incubation, the medium was replaced by acidic medium (pH 6.0) with ZGMC@ZGC-TAT (100 μg mL^{-1}). With the purpose to confirm the activated imaging property, the mouse embryonic fibroblast cell line (3T3) cells were chosen as control cells and cultured in the same way except with normal alkaline medium. After various times of incubation (2, 4, 6, 8, 10, 12, 24 h), media were discarded and PBS was added to wash cells for three times. By paraformaldehyde (4%) fixation, DAPI staining, and PBS washing, cells were observed and photographed via CLSM.

The cytotoxicity and *in vitro* CDT assay:

In order to study the cytotoxicity and CDT effects of ZGMC@ZGC-TAT, the MTT assay was carried out toward 3T3 normal cells and SCC-7 tumor cells. Firstly, 1×10^4 cells per well were planted in a 96-well cell-culture plate and incubated for 24 h. Then, the culture medium was removed and fresh medium blended with different concentration of ZGMC@ZGC-TAT (50, 100, 200, 300 μg mL^{-1}) was added and incubated for another 24 h, with SCC-7 cells cultured in acidic medium especially. Cells treated without ZGMC@ZGC-TAT was set as the control group. Then, the medium was replaced with MTT solutions (5 mg mL^{-1} in cell culture media) for 4 h. After that, 100 μL DMSO took the place of the MTT solutions, and absorbance values (at 490 nm) of each well were recorded with a microplate reader after 10 min incubation in darkness. The cell viability (%) was determined by the ratio of the absorbance of the experimental group to the absorbance of the control group.

To further confirm the CDT therapeutic efficacy, the Calcein-AM/PI staining experiment was conducted. Original medium was removed from a confocal capsule with 1×10^5 SCC-7 cells seeded and cultured for 24 h, and acidic medium (pH 6.0) containing ZGMC@ZGC-TAT (300 μg mL^{-1}) was added. In addition, other experimental groups were employed:1) 3T3 cells at pH 7.4; 2) 3T3 cells at pH 7.4 with ZGMC@ZGC-TAT (300 μg mL^{-1}); 3) SCC-7 cells at pH 6.0. After incubated for 6 h, the media were removed. Cells were washed by PBS, stained by Calcein-AM/PI staining agent, and visualized by CLSM, leading to the fluorescence confocal images records.

So as to investigate the mechanism of tumor therapy with ZGMC@ZGC-TAT,

DCFH-DA was employed as an indicator to detect the generation of intracellular ·OH. SCC-7 cells were pre-seeded in a confocal capsule (1×10^5 cells per capsule) and cultured for 24 h, followed by the removal of old medium. New acidic medium (pH 6.0), which was DMEM with neither FBS or penicillin-streptomycin, containing ZGMC@ZGC-TAT (300 μg mL^{-1}) and DCFH-DA (1×10^{-5} mol L^{-1}) was added. Also, SCC-7 cells incubated with acid DMEM, 3T3 cells incubated with alkaline DMEM containing ZGMC@ZGC-TAT (300 μg mL^{-1}) or not was set as a control group. Cultural media were discarded after being cultured for 6 h. Cells were washed by PBS for three times. Then, CLSM was used to obtain visual images of cells (λ_{ex} = 488 nm, λ_{em} = 545 nm).

Hemolysis Assay:

The mouse red blood cells (RBCs) were obtained, based on whole blood taken from BALB/c nude mice and washed with the help of centrifugation and PBS washing.

The precipitated red blood cells were prepared into 5% red blood cells solution with PBS. Then, 300 μL of 5% red blood cells solution was added into 1 mL of ZGMC@ZGC-TAT suspensions with different concentrations (50, 100, 200, 300, 400, 500, 1000 μg mL^{-1}). Deionized water and PBS served as positive and negative controls, respectively. All suspensions were incubated at room temperature for 1 h. After centrifugation at 3000 rpm for 10 min, pictures were taken and the supernatant was taken to determine the absorbance at 540 nm. The hemolysis rate was calculated according to the following equation: Hemolysis rate (%) = $(A - A_0) / (A_1 - A_0) \times 100\%$, where A, A_0 and A_1 are the absorbance values of the ZGMC@ZGC-TAT solution, negative control and positive control, respectively.

***In vivo* imaging and therapy towards lung metastasis mouse models:**

Female Balb/c athymic mice (5-6 weeks), purchased from Changzhou Cavens Laboratory Animal Co., Ltd, were used as experimental model mice. All experiments were performed abided by the law and regulation stipulation and under the authorization of Animal Ethics Committee of Jiangnan University (Protocol No: JN. No 20230530b0300831[246]). Tumor xenograft mouse model was constructed with subcutaneous injection with 1×10^6 SCC-7 cells into the right hind limb. When the diameter of the tumor on the mouse was about 6 mm, the tumor xenograft mouse model was successfully established. To establish lung metastasis (+) model, the BALB/c nude mice were injected with the suspension of 4T1 cells (1×10^6 cells per mouse) via the tail vein, and lung metastasis formed after 7 days.

In order to evaluate the intratumor imaging characteristic, the acidic tumor and alkaline muscle issue were both injected with ZGMC@ZGC-TAT (10 mg mL^{-1}, 50 μL in PBS). PL signals were acquired by a IVIS Lumina III imaging system, right after 2 min irradiation of mice with a 650 nm LED lamp, at scheduled time points (0, 2, 4, 6, 8, 10, 12, 24 h). Luminescence ratio I_{700}/I_{537} = (I_{open} - I_{537})/I_{537}, where I_{open} is PL value acquired with no emission filter applied and I_{537} was acquired only at corresponding wavelength.

Lung metastasis imaging properties was also tested. The pulmonary focal sites of mouse models were evaluated by CT imaging, along with *ex vivo* photographs and H&E staining. Lung metastasis (+) mouse model, as well as lung metastasis (-) mouse model, was injected with ZGMC@ZGC-TAT (10 mg mL^{-1}, 200 μL in PBS) intravenously.

PL signals were acquired by a IVIS Lumina III imaging system, right after 5 min irradiation of mice with a 650 nm LED lamp, at scheduled time points (0, 2, 4, 6, 8, 10, 12 h).

The lung metastasis inhibition capability was then studied. Lung metastasis (+) mice models were randomly divided into two groups, each with 6 ones. One group of mice were injected with ZGMC@ZGC-TAT (10 mg mL^{-1}, 200 μL) through tail vain, while the other group set as the control group. Mice were weighed, and sacrificed every two days. The dissected lungs were photographed, weighed and nodules counted.

To further investigate the potential systemic toxicity of ZGMC@ZGC-TAT, blood was obtained from posterior orbital vein of the mice after the treatment for blood routine examination. And then the mice were dissected and all major organs (heart, liver, spleen, lung and kidney) and tumor tissues were collected and fixed with 4% formaldehyde for H&E staining.

Supplementary References.

1 J. Wang, Q. Ma, W. Zheng, H. Liu, C. Yin, F. Wang, X. Chen, Q. Yuan, W. Tan, *ACS Nano*, 2017, **11**, 8185–8191.

2 X. Zhao, X. Wei, L.-J. Chen, X.-P. Yan, *Biomater. Sci.*, 2022, **10**, 2907–2916.

3 L.-J. Chen, X. Zhao, X.-P. Yan, *ACS Appl. Mater. Interfaces*, 2019, **11**, 19894–19901.

4 X. Wei, X. Huang, Y. Zeng, L. Jing, W. Tang, X. Li, H. Ning, X. Sun, Y. Yi, M. Gao, *ACS Nano*, 2020, **14**, 12113–12124.

5 X.-M. Gao, T.-Y. Gu, K.-L. Chen, X. Zhao, X.-P. Yan, *Analysis & Sensing*, 2023, **4**, e202300045.

6 Y. Li, C.-X. Yang, X.-P. Yan, Chem*. Commun.*, 2017, **53**, 2511–2514.

Supplementary Figures

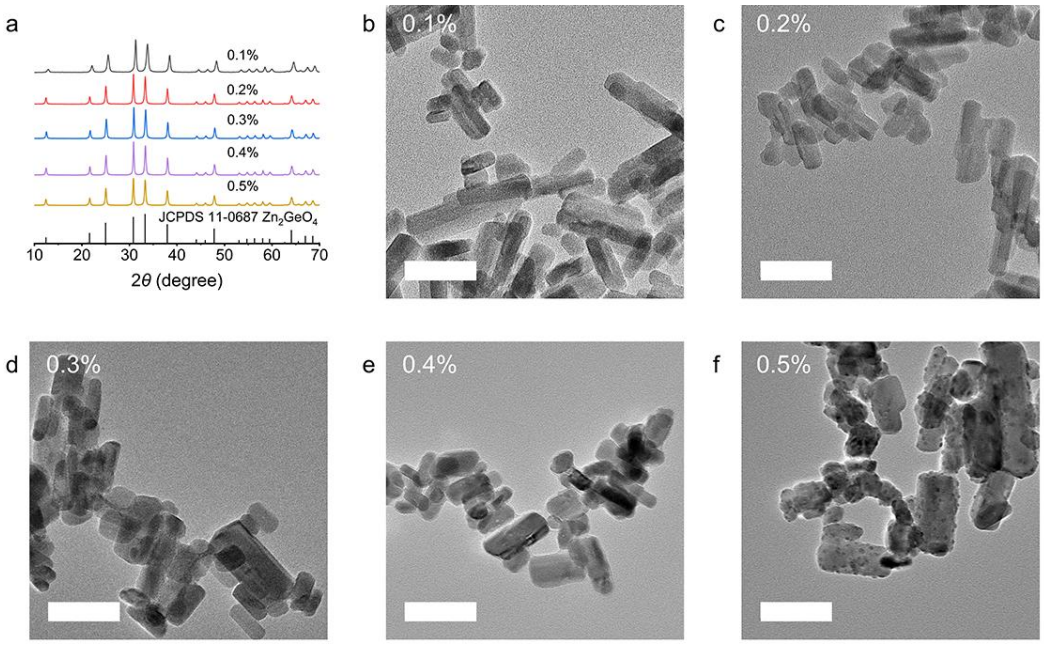

Figure S1. (a) corresponding XRD patterns and (b-f) TEM images of ZGMC synthesized with various doping amount of Cu^{2+} (Scale bar, 100 nm).

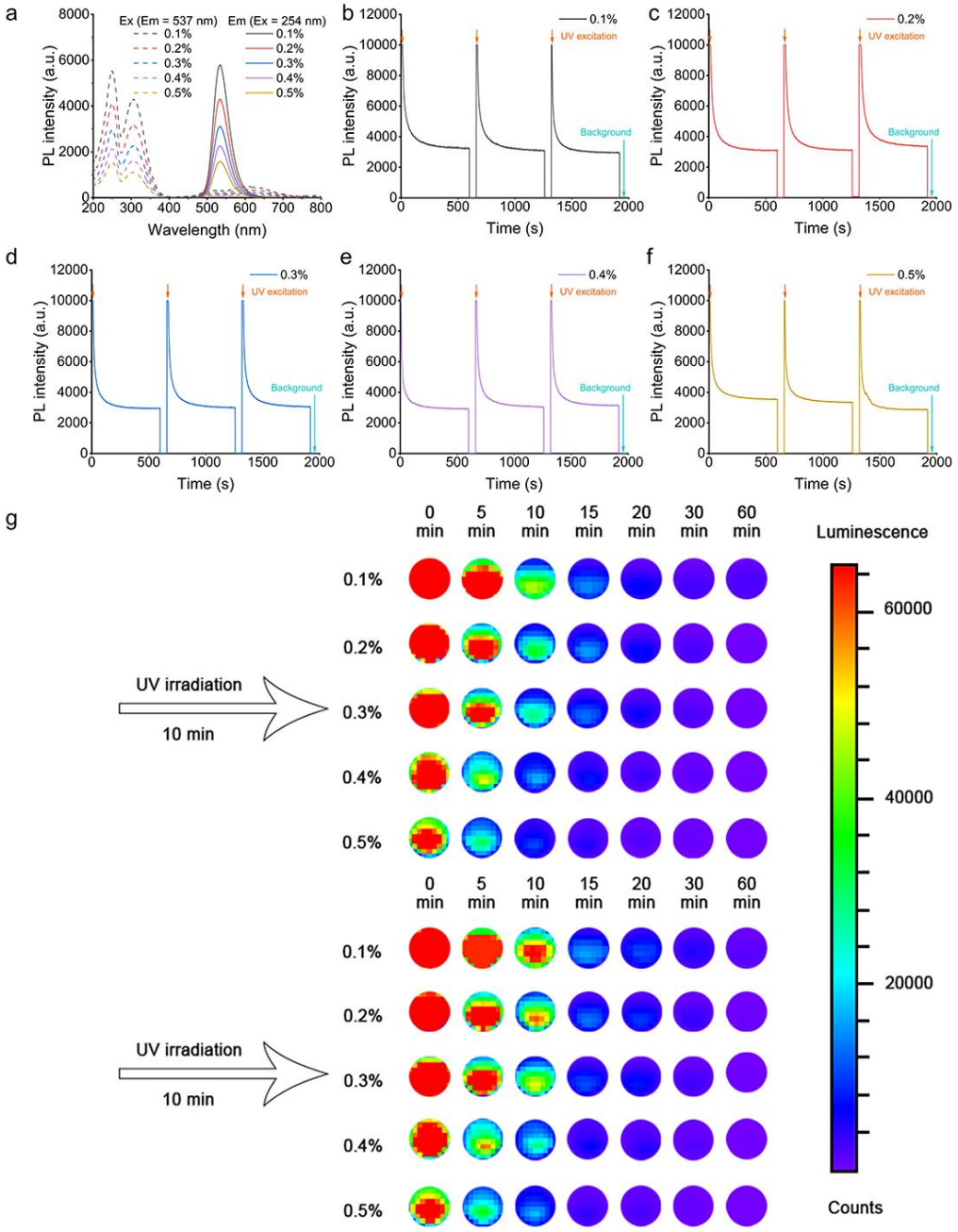

Figure S2. (a) Phosphorescence spectra and (b-f) afterglow decay curves recorded on a fluorescence spectrophotometer and (g) recorded on a Lumina III imaging system of ZGMC with various doping amount of Cu^{2+} after 254 nm UV irradiation for 10 min.

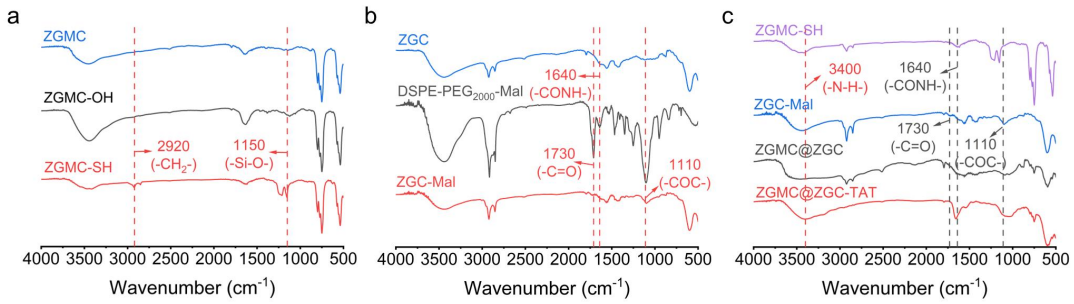

Figure S3. (a) FT-IR spectra of ZGMC, ZGMC-OH and ZGMC-SH. (b) FT-IR spectra of ZGC, DSPE-PEG$_{2000}$-Mal and ZGC-Mal. (c) FT-IR spectra of ZGMC-SH, ZGC-Mal, ZGMC@ZGC, and ZGMC@ZGC-TAT.

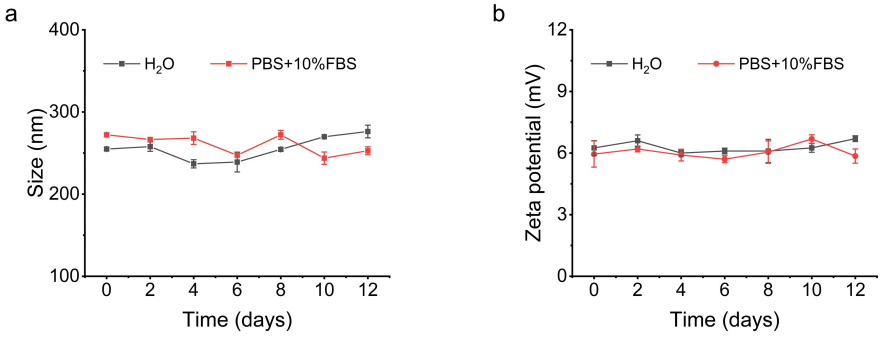

Figure S4. (a) Hydrodynamic size distribution and (b) Zeta potential changes of ZGMC@ZGC-TAT in 12 days. Center values and error bars are defined as mean ± SD, respectively (n = 3).

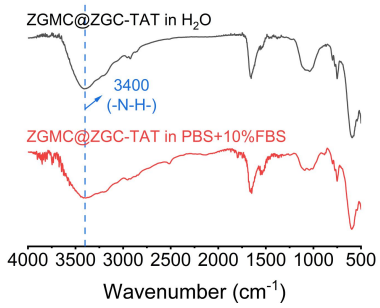

Figure S5. FT-IR spectra of ZGMC@ZGC-TAT in H_2O and PBS + 10% FBS, respectively, after 12 days.

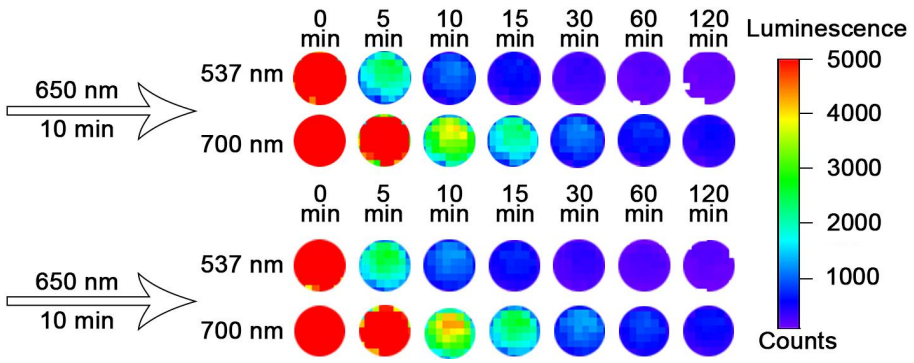

Figure S6. PL images of ZGMC@ZGC-TAT recorded on Lumina III imaging system.

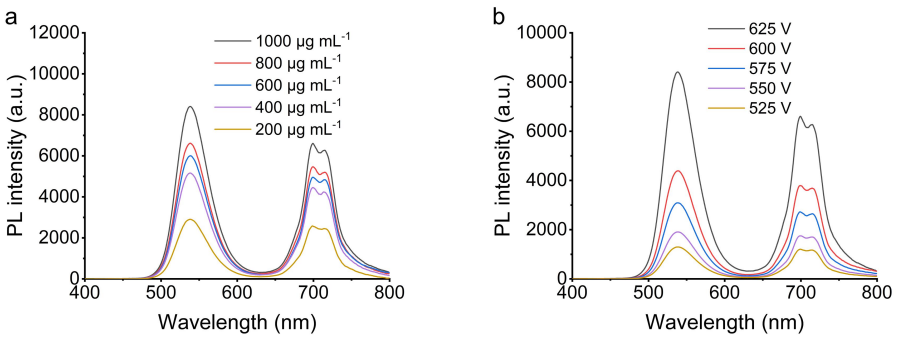

Figure S7. Emission (excitation at 254 nm) spectra of ZGMC@ZGC-TAT (a) of different concentration (625 V) and (b) at different test voltage (1000 μg mL^{-1}).

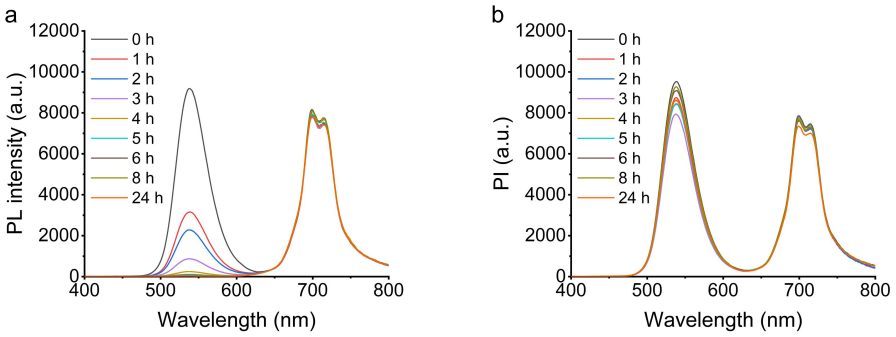

Figure S8. Time-dependent phosphorescence change curves of ZGMC@ZGC-TAT at (a) pH 6.0 and (b) pH 7.4.

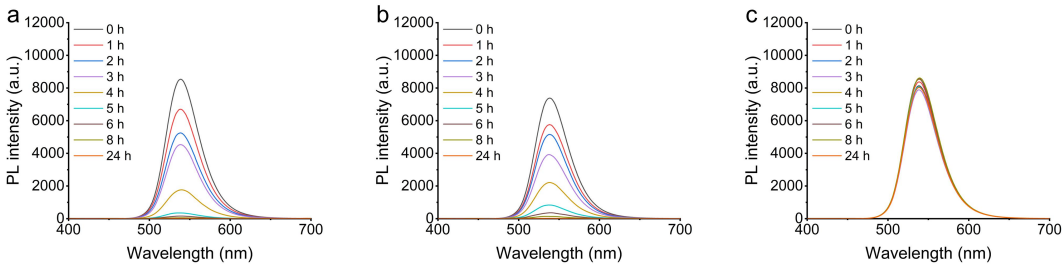

Figure S9. Time-dependent phosphorescence change curves of ZGMC at (a) pH 6.0, (b) pH 6.5, and (c) pH 7.4.

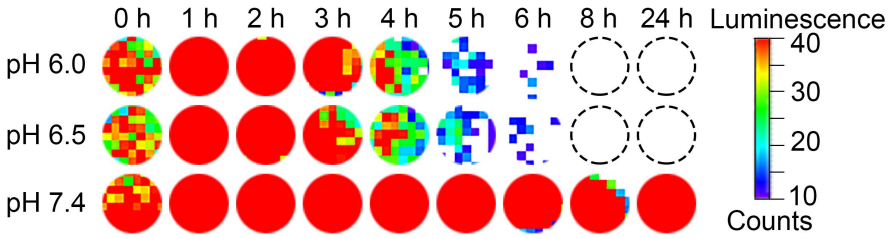

Figure S10. Phosphorescence of ZGMC (600 μg mL^{-1}) in different pH solutions at different times recorded on a Lumina III imaging system after 10 min 254 nm UV irradiation.

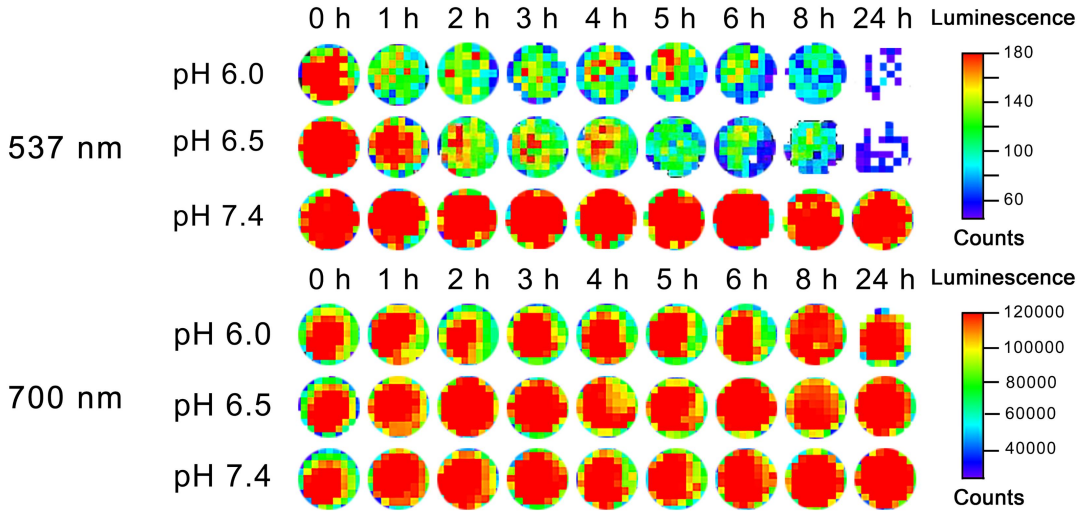

Figure S11. Phosphorescence of ZGMC@ZGC-TAT (600 μg mL^{-1}) in different pH solutions at different times recorded on a Lumina III imaging system after 10 min 254 nm UV irradiation.

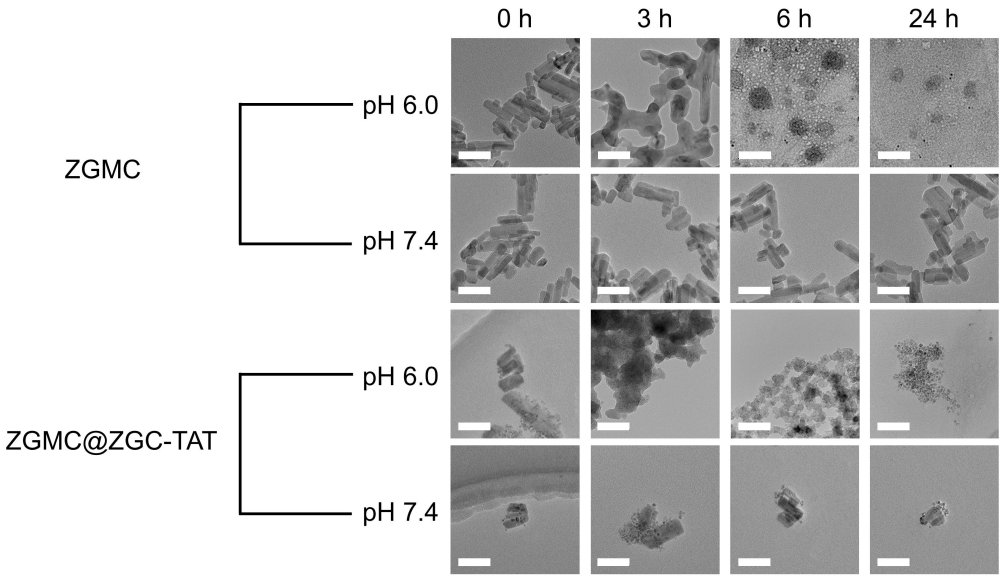

Figure S12. TEM images of ZGMC and ZGMC@ZGC-TAT at different pH in different times (Scale bar, 100 nm).

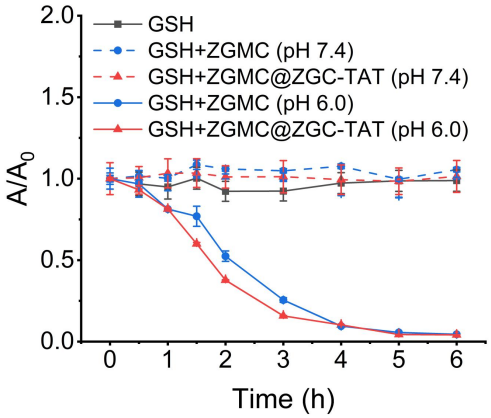

Figure S13. Time-dependent absorbance of different DTNB solutions at 410 nm (A/A_0). A_0 and A are the absorbances of DTNB solutions before reaction and after reaction at a certain time, respectively.

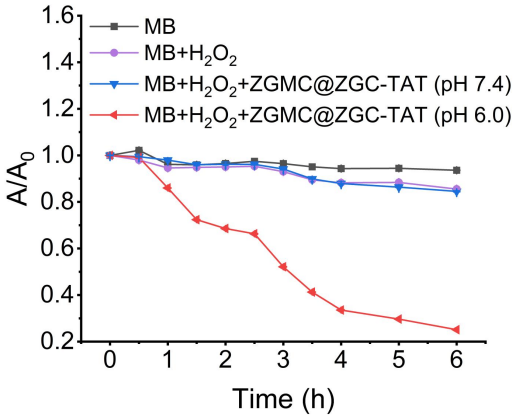

Figure S14. Time-dependent absorbance of different MB solutions at 664 nm (A/A_0). A_0 and A are the absorbances of MB solutions before reaction and after reaction at a certain time, respectively.

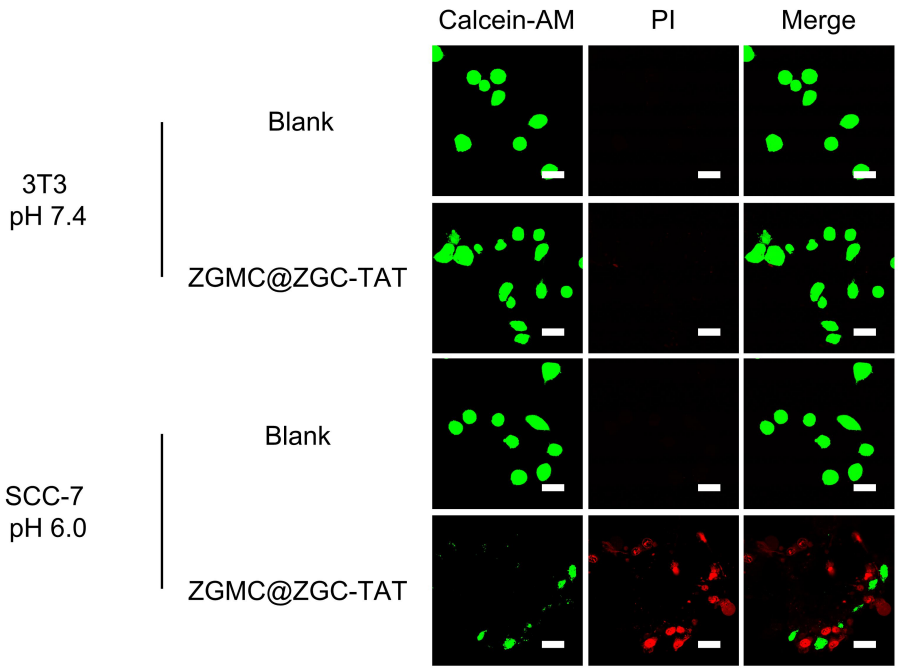

Figure S15. Live/dead staining of 3T3 and SCC-7 cells treated with or without 300 μg mL^{-1} ZGMC@ZGC-TAT (scale bar, 30 μm).

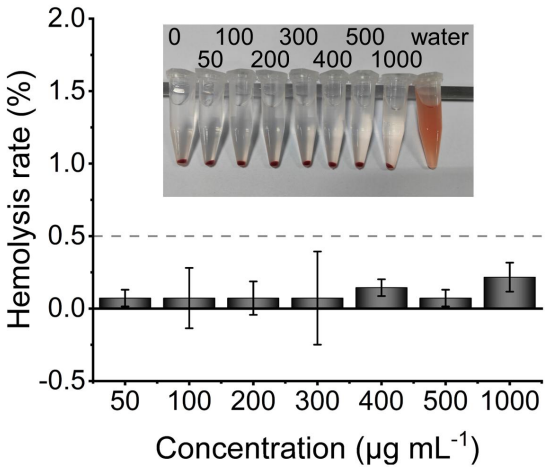

Figure S16. Hemolysis rate of red blood cells incubated with ZGMC@ZGC-TAT at various concentrations. The insert is the corresponding photograph of red blood cells with different treatments. Center values and error bars are defined as mean ± SD, respectively (n = 3).

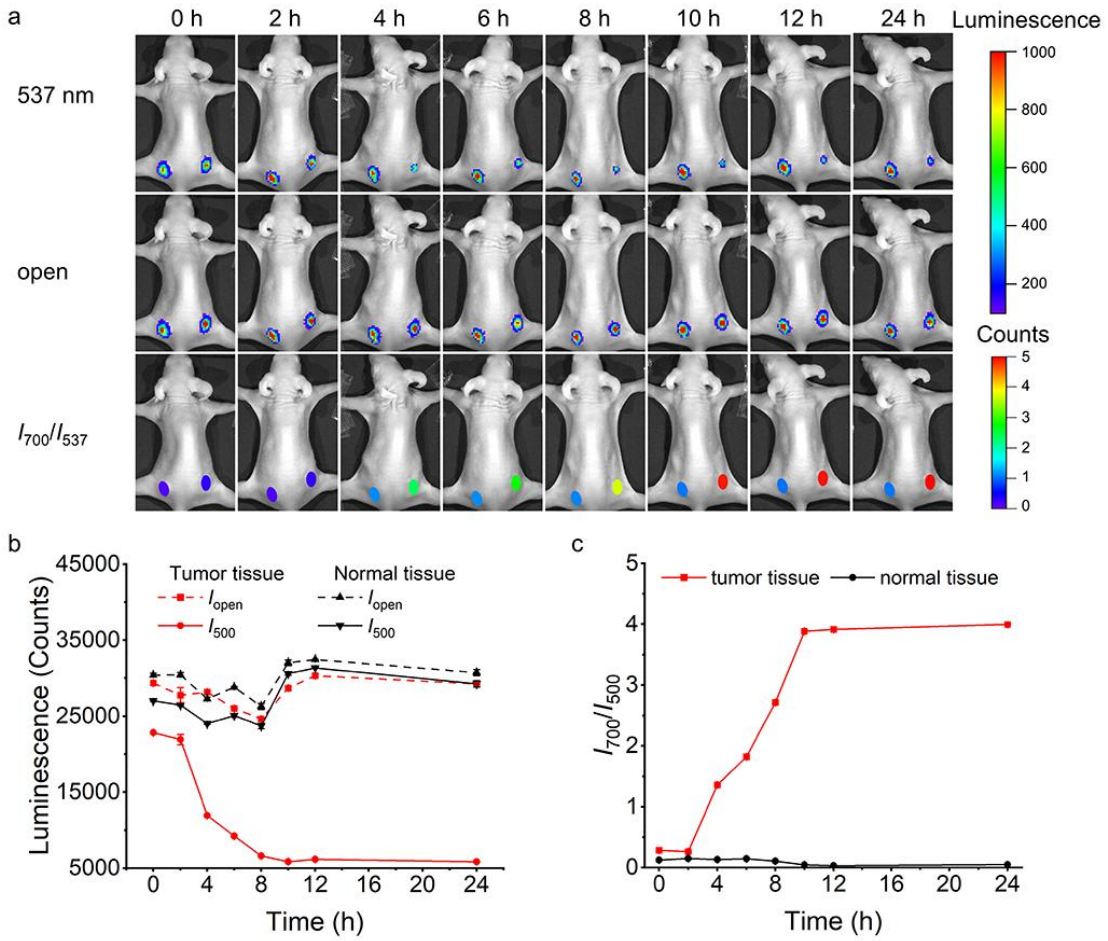

Figure S17. (a) *In vivo* phosphorescence images of SCC-7 tumor xenograft mice throughout time, (b) luminescence intensity and (c) luminescence ratio I_{700}/I_{537} at tumor and normal tissues at different times after intratumor injection of ZGMC@ZGC-TAT in SCC-7 tumor xenograft mice.

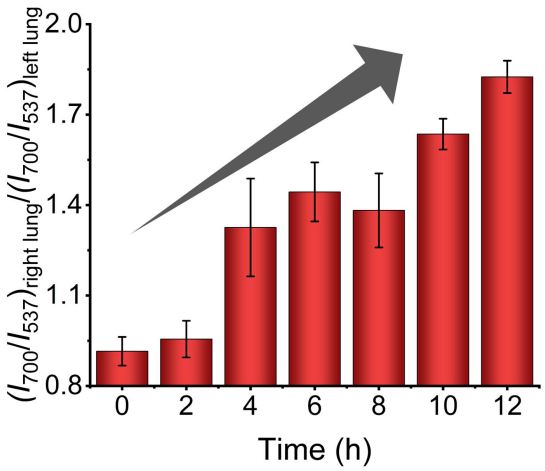

Figure S18. I_{700}/I_{537} ratio between right and left lungs of lung metastasis (+) models at different times after intravenous injection of ZGMC@ZGC-TAT.

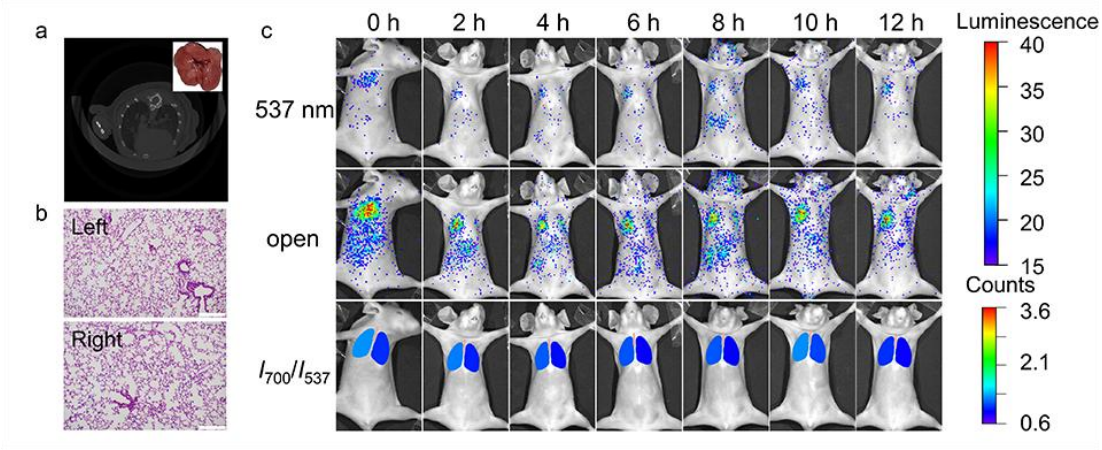

Figure S19. (a) CT image and *ex vivo* photograph (inset) of lung metastasis (-) mice models. (b) H&E staining of left and right lungs (Scale bar, 200 μm). (c) *In vivo* luminescence images of lung metastasis (-) mice models after intravenously injected with ZGMC@ZGC-TAT throughout time.

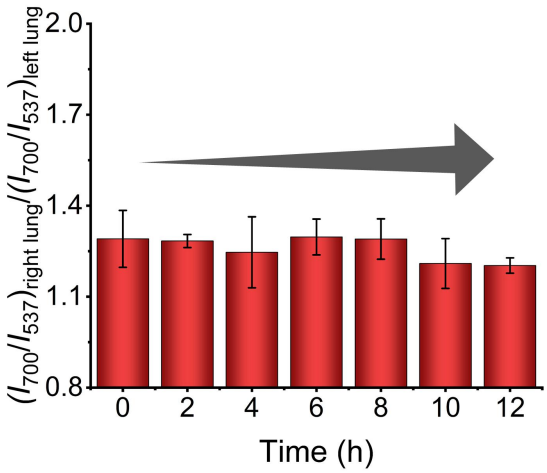

Figure S20. I_{700}/I_{537} ratio between right and left lungs of lung metastasis (-) mice models at different times after intravenous injection of ZGMC@ZGC-TAT.

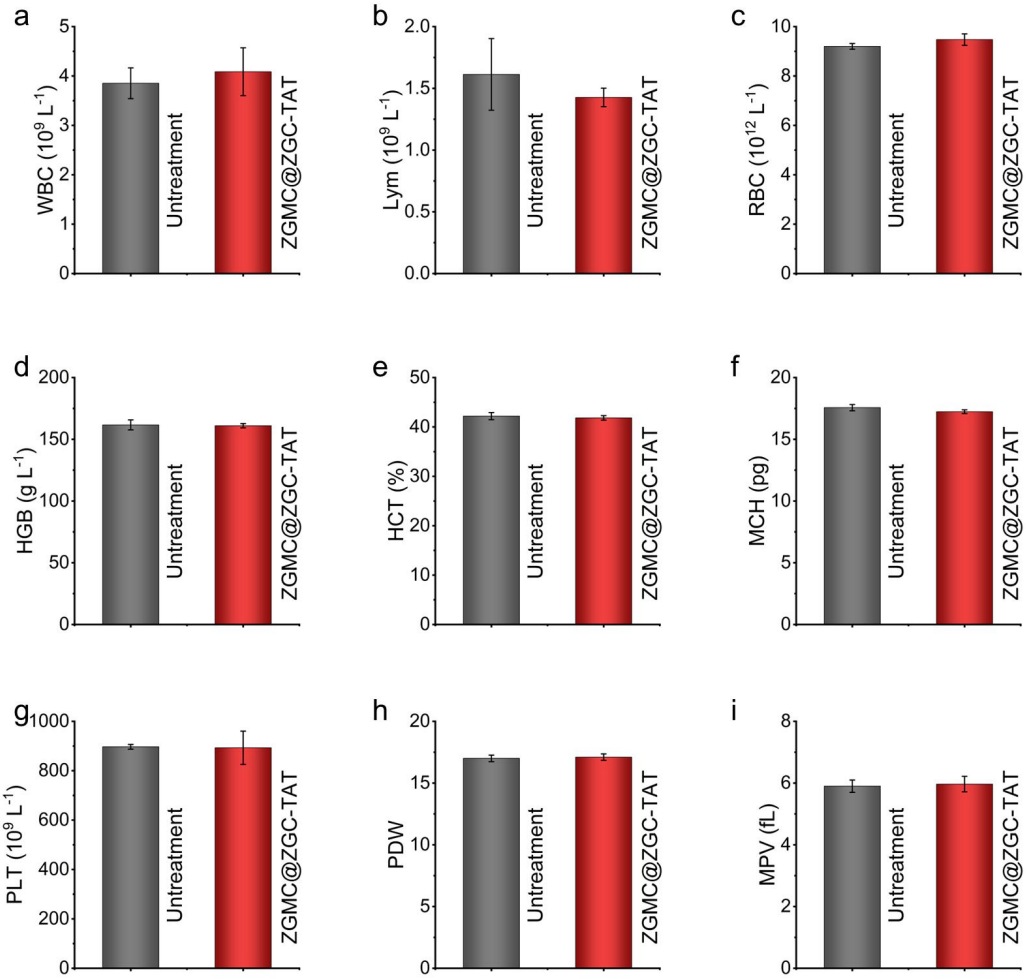

Figure S21. Blood routine examination of mice after different treatments: (a) white blood cells (WBC); (b) lymphocyte (Lym); (c) red blood cells (RBC); (d) hemoglobin (HGB); (e) hematocrit (HCT); (f) mean corpuscular hemoglobin (MCH); (g) platelets (PLT); (h) platelet distribution width (PDW); (i) mean platelet volume (MPV).

Supplementary Tables

Table S1. Elemental content of Mn/Cu in ZGMC with various doping amount of Cu^{2+}

Doping amount of Cu^{2+} (%)	Mn content (nmol mL^{-1})	Cu content (nmol mL^{-1})	Mn + Cu content (nmol mL^{-1})
0.1	3.8507 ± 0.0056	0.0694 ± 0.0004	3.9201 ± 0.0060
0.2	3.7941 ± 0.0021	0.1412 ± 0.0004	3.9354 ± 0.0025
0.3	3.6249 ± 0.0042	0.1758 ± 0.0007	3.8007 ± 0.0049
0.4	3.4330 ± 0.0001	0.2891 ± 0.0002	3.7221 ± 0.0002
0.5	3.2155 ± 0.0033	0.3873 ± 0.0005	3.6028 ± 0.0038